International Journal of Scientific Research in Science and Technology
Print ISSN: 2395-6011 | Online ISSN: 2395-602X (www.ijsrst.com)
© 2021 | IJSRST | Volume 8 - Issue 1

Synthesis and Luminescence Properties of LaB_3O_6 Doped with Eu^{3+}, Dy^{3+} and Tb^{3+}

Varsha Rangari[1], J.G. Mahakhode[2*], Yatish R. Parauha[3], S J Dhoble[3]
[1]Department of Electronics, Dharampeth M. P. Deo Memorial Science College, Nagpur, Maharashtra, India
[2]Department of Electronics, Dhote Bandhu Science College, Gondia, Maharashtra, India
[3]Department of Physics, R.T.M. Nagpur University, Nagpur, Maharashtra, India
*Corresponding author email: jayantmahakhode@gmail.com

ABSTRACT

In the present investigation, photoluminescence properties of rare earth doped LaB_3O_6 phosphors were investigated. Eu^{3+}, Dy^{3+} and Tb^{3+} are used as rare earth ions for this investigation. Series of Eu^{3+}, Dy^{3+} and Tb^{3+} doped LaB_3O_6 phosphors were synthesized sing solid state diffusion method. Powder X-ray diffraction technique (XRD) along with CIE color coordinates including their PL properties with emission intensity effect too were analyzed for the characteristics of prepared phosphors. Effect of heating time during synthesis and concentration of Eu^{3+} on PL properties of LaB_3O_6 was investigated and observed that increasing the heating time of synthesis changes the emission of Europium from blue to red i.e. Eu^{2+} to Eu^{3+}. The emission spectra of Dy^{3+}: LaB_3O_6 phosphors show two strong bands in blue and yellow regions and can be useful for solid state lighting in lamp industry. LaB_3O_6: Tb^{3+} may be predicted as a promising green phosphor candidate for applications in LED based solid state lighting or other display devices because of its excitation at 379nm.

Keywords :- Solid state method, X-ray diffraction technique (XRD), Photoluminescence, CIE, LED

I. INTRODUCTION

With the development of society, people requirements for display and relative light source are increasing continuously. Therefore from the past few years, much attention has been paid to the study of vacuum ultraviolet (VUV) and ultraviolet (UV) phosphors due to the demand of Plasma Display Panels (PDPs), emission Displays (FEDs) and light Emitting diodes (LEDs) [1–3]. To fulfill these requirements, high power light source such as high power LEDs and LASER (Light Amplification by Stimulated Emission of Radiation) has gradually become the research hotspot. Modern optoelectronic devices require phosphor materials (luminophores) to convert UV or near UV blue radiation into light. Lanthanide doped compounds have played outstanding roles as phosphors in lighting, flat panel displays, optical telecommunication, and as active materials in solid state lasers [4–6]. There are different kind of inorganic phosphors based on lanthanides such as oxides, silicates, aluminates (garnets), phosphates and borates. The last group rare earth borate phosphor is recently studied and reveals quite promising. Borate based compounds are of high

chemical and photolytic stability and can be efficiently doped with Eu^{3+}, Tb^{3+}, Nd^{3+} and other lanthanide ions. Lithium tetra borate $Li_2B_4O_7$ (LTB) was the first borate synthesized in England [7]. About 65% of known borate compounds have crystallo chemical structures characterized by BO_3 triangles which are either isolated or joined with each other. Such anionic units form ionic bonds with metal cations. Such structures are typically ortho, pyro and meta borates. In polyborates, the triangles are joined both with each other and with tetrahedrons by the common oxygen atom [8]. A large number of borate compounds are transparent over a wide spectral range, beginning from VUV and extending into infrared (IR). This is one of the reasons that borate compounds become important optoelectronics materials. Many researches are studying borate compound based materials for nonlinear optics, acousto electronics, piezotechnique and dosimeter and also because of large band gap, they are good choice as host lattices for luminescent ions. Borate compounds like BaB_2O_4 [9], LiB_3O_5 [10], $CsLiB_6O_{10}$ [11] and $K_2Al_2B_2O_7$ [12] possess high non-linear optical (NLO) coefficient. Eu^{3+} and Tb^{3+} doped borates are often used as luminescent materials, because of their optimized properties which allow them to withstand the harsh condition in vacuum discharge lamps or screens. Rare earth doped borate phosphors have applications in various fields. Rare earth doped $Ca_4GdO(BO_3)_3$ [13,14] compounds are important solid state laser materials. $YAl_3(BO_3)_4$ doped with Nd^{3+} [15], as well as the 3d transition impurities also find applications in solid state lasers. $Li_2B_4O_7$ can be useful for VUV laser [16]. $Li_2B_4O_7$: Cu^{2+} [17] , and MgB_4O_7:Dy^{3+} [18] phosphors are used in commercial dosimetry systems based on thermoluminescence. $Sr_2B_5O_9Cl$: Eu also exhibits promising dosimetric characteristics [19]. Europium doped alkaline haloborates are also considered for the neutron radiography using photo stimulated luminescence (PSL). $(Gd_{0.6}Ce_{0.2}Tb_{0.2})MgB_5O_{10}$ is a green emitting phosphor used in the tricolour lamps [20]. SrB_4O_7:Eu^{2+} phosphor is used in commercial sun tanning lamps [21]. $(La,Gd)B_3O_6$: Bi is another borate based, UV emitting phosphor of commercial importance [22]. Cathodoluminescent phosphor $InBO_3$:Tb^{3+} is used as a green emitting phosphor in projection color TV; application in neutrino detection has also been suggested [23], while Tb doped $(Y,Gd)BO_3$ finds place as green emitting phosphor for plasma display panels (PDP) [24]. Other barium containing borates such as $Ba_5(B_2O_5)_2F_2$ [25] are good hosts for RE^{2+}, while the RE stoichiometric borates are promising hosts for trivalent rare earth ions. Borate based luminophors may be applied in different devices like luminescent tubes and plasma display panels as well as LEDs. Borate phosphors are usually reported to be good luminescent material for plasma display panels [26]. Now a day, however it seems to be important to develop near UV to visible phosphors aimed for application in LED. In phosphor converted LEDs commercially available InGaN and GaN LED chips (420-480 nm and 360-370 nm, respectively) [4] are used as light source for phosphors excitation. This paper reports the synthesis of two borate compounds i.e. LaB_3O_6 doped with different concentrations of Eu^{3+}, Dy^{3+} and Tb^{3+} using the high temperature solid state diffusion method. It also reports the investigations of synthesized borates morphology, structural and luminescence properties in detail, based on X-ray diffraction (XRD) profile and photoluminescence. CIE Color coordinates of prepared phosphors with standard one have also been reported.

II. Synthesis

The powder samples $La_{(1-x)}B_3O_6Eu_x$ (x=0.05,0.1,0.2,0.5,1m%) were synthesized using a solid state diffusion technique at high temperature. The starting materials used are of analytical grade La_2O_3, H_3BO_3 and rare earth oxide Eu_2O_3. The stoichiometric reactants were mixed and ground thoroughly in an agate mortar with acetone to get homogeneous mixture. Then the mixtures were heated at 800° C for

24 hrs and 48 hrs under air atmospheres. The final products were cooled down to room temperature and ground again into powder for further characterization. Other series of samples $La_{(1-x)}B_3O_6Ln_x$ (Ln = Dy, Tb and x=0.05,0.1,0.2,0.5,1m%) were synthesized by the same method at 800°C for 24 hrs.

The final products were cooled down to room temperature and ground again into powder for further characterization.

III. Measurements

The Phase of the prepared phosphor was examined by XRD with Cu-Kα (λ= 15418Å) radiation at 40 kV and 30 mA. The photoluminescence measurements were carried out using Shimadzu RF-5301 PC fluorescence spectrophotometer equipped with a 150W Xenon lamp as the excitation source at room temperature and setting the excitation and emission slits at 1.5 nm. The Commission International de I'Eclairage (CIE) color co-ordinates were obtained using Radiant Imaging color calculator software.

IV. Results and discussion

4.1 Phase identification and morphology

In order to check the phase purity and phase structure, powder XRD measurements were carried out. Figure 1 shows the XRD pattern of LaB_3O_6: Eu^{3+} phosphor. The entire diffraction peaks are in good agreement with those in JCPDS file no. 01-073-1150, indicating that the obtained sample is single phase. The pattern exhibit the formation of single-phase compound with the monoclinic structure belonging to the I2/a space group with lattice parameter (a=7.9560Å, b=8.172 Å, c= 6.4990 Å, β=93.6300 Å), without any secondary or impurity phases.

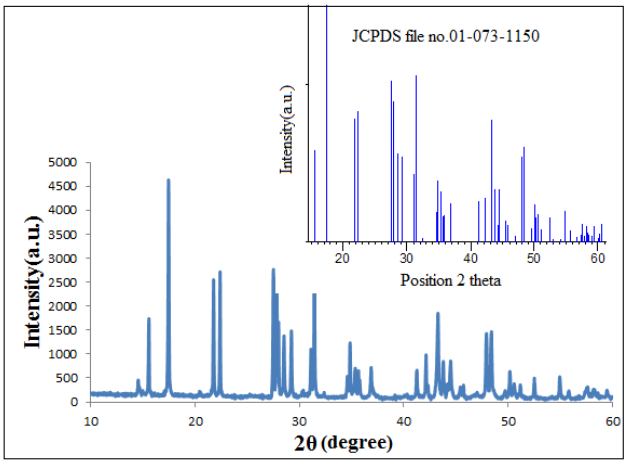

Figure 1 : XRD pattern of LaB_3O_6: Eu and JCPDS standard card no. 01-073-1150.

4. 2 Infra red spectral analysis

To analyze the presence of functional groups in LaB_3O_6 qualitatively, we recorded Fourier transform infra-red (FTIR) spectrum in the range 375- 3975 cm^{-1} using Shimadzu IR affinity-1 infrared spectrometer (Figure 2). The bands observed in the 900-1350 cm^{-1} region in the FTIR spectrum are characteristics of BO_3 asymmetric and symmetric stretching vibrations and are in agreement with other compounds containing BO_3 anionic groups [27,28]. The bands observed between 400 and 750cm^{-1} are attributed to the bending vibrations of the BO_3 and BO_4 groups.

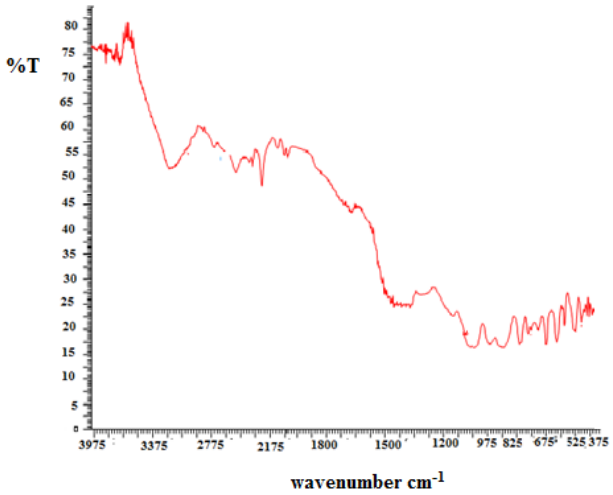

Figure 2 : Infra-red spectra of Eu^{3+} doped LaB_3O_6

4.3 Luminescence properties

4.3.1 LaB_3O_6: Eu^{3+} phosphor

The excitation spectrum of $La_{0.99}B_3O_6Eu_{0.01}$ prepared at 800° C for 24 hrs, 48 hrs and quenched at 800°C for 1 hr, using solid state diffusion method is shown in figure 3 (a, b and c). It shows broad excitation band in the wavelength range 220 nm to 300 nm peaking at 263 nm, which can be attributed to the charge transfer from O^{2-} to Eu^{3+}. The charge transfer from O^{2-} to Eu^{3+} in $La_{0.99}B_3O_6Eu_{0.01}$ lattice is observed very strong. Apart from the charge transfer band, some sharp lines were also seen in the excitation spectrum of Eu^{3+} with host, which corresponds to the f-f transitions, all originated from transitions within Eu^{3+} $4f^6$ configuration [29]. Increasing the heating time decreases the intensity of CT band and all other excitation peaks as shown in figure 3. Very few trivalent lanthanide's f-f transitions are sensitive to the environment and become more intense but mostly of them are not affected by the environment. Such transitions have been called hypersensitive transitions [30]. This luminescence feature can yield structure information of a different character from that obtained by X-ray diffraction. All emission spectra were normalized to the intensity of the $^5D_0 \rightarrow {}^7F_1$ magnetic dipole transition, which is known to be largely independent on the environment of Eu^{3+} ion. The $^5D_0 \rightarrow {}^7F_0$ emission is a strictly forbidden transition with the selection rule $D_J = 0$, if Eu^{3+} ion occupies an inversion symmetry site in the crystal lattice [2,30]. The magnetic dipole transitions $^5D_0 \rightarrow {}^7F_1$ are insensitive to the site symmetry, because they are parity-allowed. Particularly, the forced electric dipole transition $^5D_0 \rightarrow {}^7F_2$ with $D_J = 2$ is hypersensitive, and the intensity can vary by orders of magnitude, depending on the local site symmetry [2,30]. Upon excitation at 395 nm, the Eu^{3+} ions are promoted from the ground state to $^5L_6$ state and relax to $^5D_0$ energy level following a non- radiative process. The $^5D_0$ level is populated and thus responsible for the fluorescence at ^7F_J (J = 0–2) energy levels.

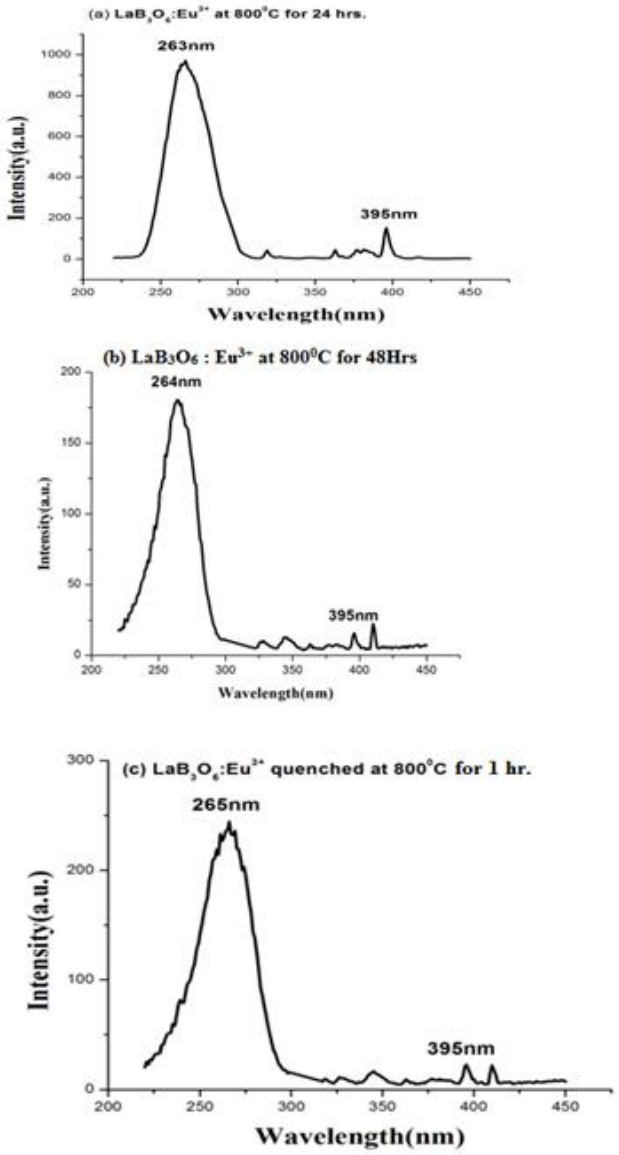

Figure 3: Excitation spectra of sample LaB_3O_6:Eu^{3+} prepared (a) at 800° C for 24 hrs, (b) at 800° C for 48 hrs and (c) quenched at 800° C for 1 hr.

The emission spectrum of Eu^{3+} doped LaB_3O_6 prepared at 800°C for 24 hrs and 48 hrs is shown in figure 4 and 5 respectively. Figure 6 shows the emission spectrum of Eu^{3+} doped LaB_3O_6 quenched at 800°C for 1 hr. It is seen from figure 4 and 5 that with increase in temperature, Eu changes from Eu^{2+} to Eu^{3+}. It can be seen from figure 5 and 6, the stark splittings of the $^5D_0 \rightarrow {}^7F_0$, $^5D_0 \rightarrow {}^7F_1$ and $^5D_0 \rightarrow {}^7F_2$ emission lines are 1(580 nm), 3 (588, 592 and 599 nm) and 2 (616 and 624 nm), respectively. The strongest emission peak situated at 588 nm showing prominent and bright orange spectra is due to the

magnetic dipole transition $^5D_0 \rightarrow {}^7F_1$. A peak at 610 nm can be attributed to Eu^{3+} forced electric dipole transition $^5D_0 \rightarrow {}^7F_2$. It is relatively weak, which indicates the Eu^{3+} site has inversion symmetry and $^5D_0 \rightarrow {}^7F_0$ electric dipole transition is very weak.

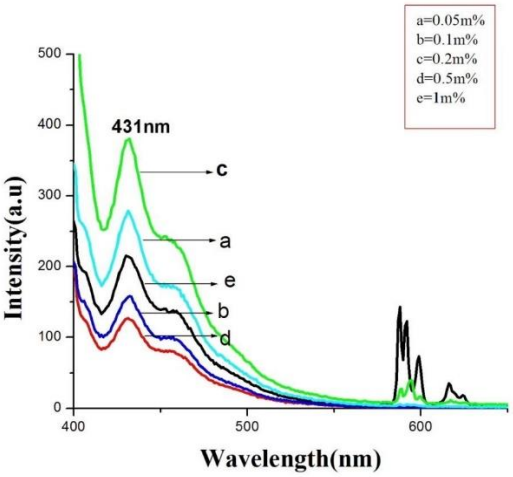

Figure 4 : Emission spectra of sample $LaB_3O_6:Eu^{3+}$ prepared at 800° C for 24 hrs.

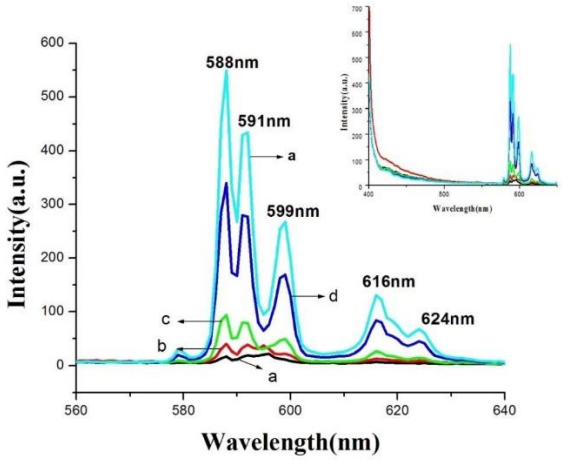

Figure 5 : Emission spectra of sample $LaB_3O_6:Eu^{3+}$ prepared at 800° C for 48 hrs.

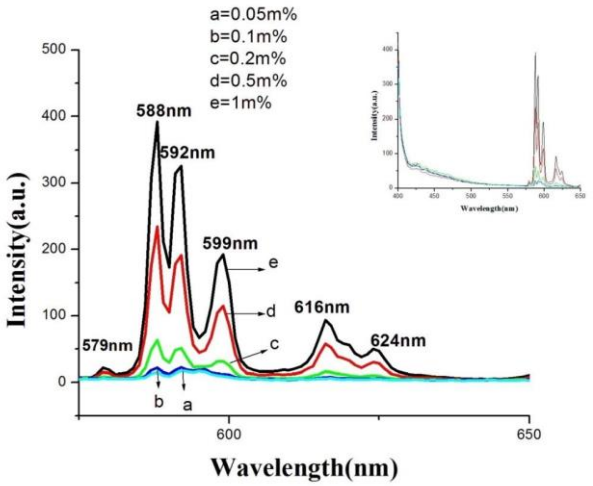

Figure 6 : Emission spectra of sample $LaB_3O_6:Eu^{3+}$ quenched at 800° C for 1 hr.

The maximum splitting of the F_J levels for a given site is (2J+1) where J is the angular momentum. Figure 7 shows the emission mechanism of Eu^{3+} ion showing stark splitting in LaB_3O_6 phosphors under 395nm excitation. In general, when the Eu^{3+} ion is located at crystallographic site without inversion symmetry, its hypersensitive forced electric-dipole transition $^5D_0 \rightarrow {}^7F_2$ red emission dominates in the emission spectrum. If the Eu^{3+} site possesses an inversion center, $^5D_0 \rightarrow {}^7F_1$ orange emission is dominant. The distinct emission lines between 580 and 650nm are observed due to transitions from excited $^5D_0$ to the ^7F_J (J = 0–3) levels of Eu^{3+} ions. The origin of these transitions (electric dipole or magnetic dipole) from emitting levels to terminating levels depend upon the location of Eu^{3+} ion in LaB_3O_6 lattice and the type of transition is determined by selection rule [31]. The most intense peak in the vicinity of 588 nm is ascribed to the magnetic dipole transition of $^5D_0$ and $^7F_1$ levels. The weak emission at 616 and 624 nm corresponds to the hypersensitive transition between the $^5D_0$ and $^7F_2$ levels due to forced electric dipole transition mechanism. The presence of unique emission line at 580 nm ($^5D_0 \rightarrow {}^7F_0$) indicates that Eu^{3+} occupies only one site in the lattice. The presence of both ED and MD electronic transitions in the emission spectra confirms that the site occupied

by Eu^{3+} in this host i.e LaB_3O_6 is not strictly Centro symmetric.

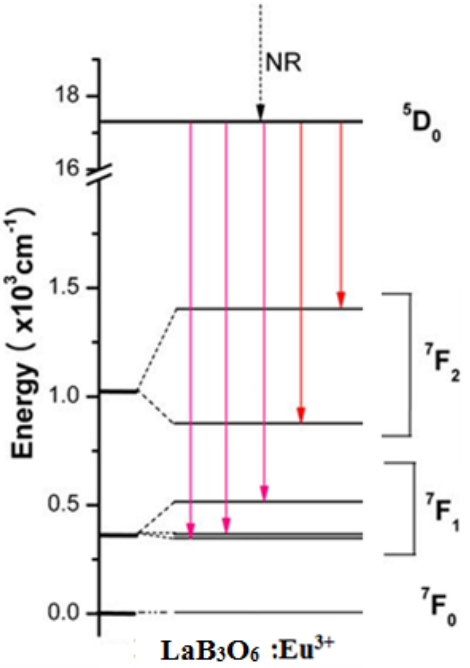

Figure 7 : Emission mechanism of Eu^{3+} ion showing stark splitting in LaB_3O_6 phosphors under 395nm excitation.

4.3.2 LaB_3O_6: Dy^{3+} phosphor

In general there are nine obvious excitation peaks of Dy^{3+}, and are assigned to the transitions from the ground level $^6H_{15/2}$ to higher levels based on the energy levels reported by Carnall et al. [32]. Figure 8 shows the excitation spectra of Dy^{3+} doped LaB_3O_6 phosphor. The excitation spectra shows the peak at 348 nm which have been assigned to the transition from the ground level $^6H_{15/2}$ to higher levels $^6H_{15/2} \rightarrow {}^6P_{7/2}$ of Dy^{3+} [59]. At 348nm excitation, emission spectrum was measured in the 400–650nm range as shown in figure 9. The emission spectra have similar pattern for all the as-prepared samples. Two emission peaks at 475nm (blue) and 575nm (yellow) are corresponding to $^4F_{9/2} \rightarrow {}^6H_{15/2}$ and $^4F_{9/2} \rightarrow {}^6H_{13/2}$ transitions of Dy^{3+} ion, respectively. The $^4F_{9/2} \rightarrow {}^6H_{15/2}$ transition has mainly been magnetically allowed and hardly varies with the crystal field strength around the Dy^{3+} ions [33]. The $^4F_{9/2} \rightarrow {}^6H_{13/2}$ transition is a forced electric dipole transition being allowed only at low symmetries with no inversion centre [33].

Figure 10 shows the dependence of the luminescence intensity at 475 nm with the dopant ion Dy^{3+} concentration. The pattern of emission spectrum does not vary with the Dy^{3+} concentration but the luminescence intensity changes more significantly. It can be found that the emission intensity of Dy^{3+} increases with an increase of dopant ion concentration (x), it reaches to a maximum value at x = 0.01, and then decreases with an increase of dopant (x) due to concentration quenching [33]. The reason must be that when the concentration of Dy^{3+} continues to increase, the interaction increases and leads to self-quench. Therefore the emission intensity decreases. The concentration quenching of Dy^{3+} luminescence is mainly caused by cross-relaxation, i.e. energy transfers from one Dy^{3+} to another neighbor Dy^{3+} by transition that match in energy. These transitions are mainly Dy^{3+} ($^4F_{9/2}$) + Dy^{3+} ($^6H_{15/2}$) → Dy^{3+}($^6F_{3/2}$) + Dy^{3+} ($^6F_{11/2}$) [34,35].

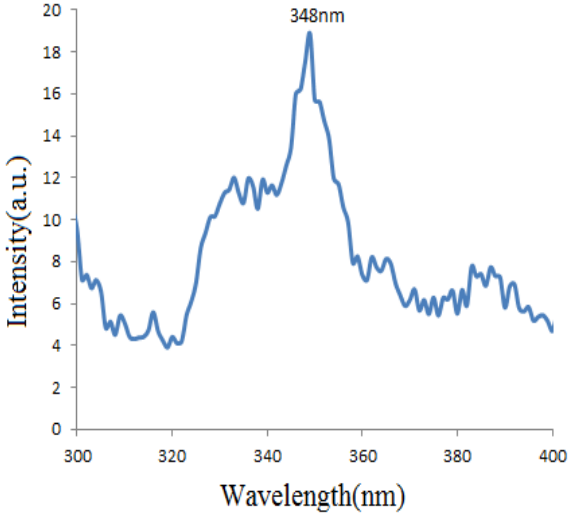

Figure 8 : Excitation spectrum of LaB_3O_6 :Dy^{3+}.

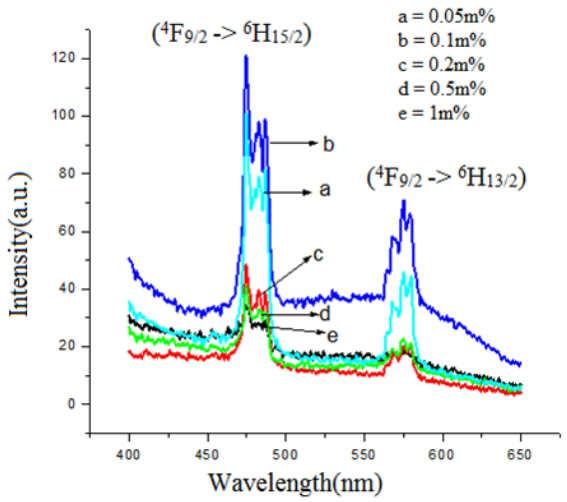

Figure 9 : Emission spectrum of LaB_3O_6 :Dy^{3+} λ_{ex}=348nm.

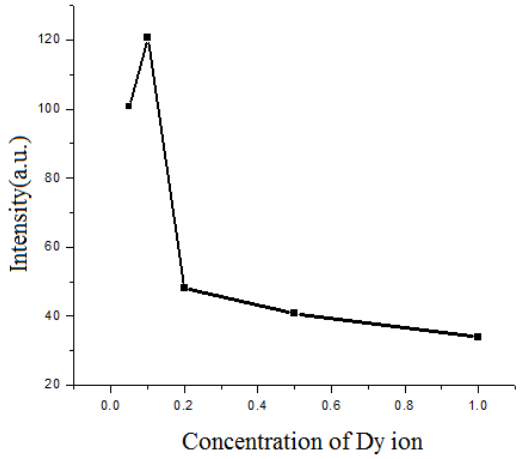

Figure 10 : Effect of concentration of doped Dy^{3+}on relative luminescent intensity for LaB_3O_6: Dy^{3+}.

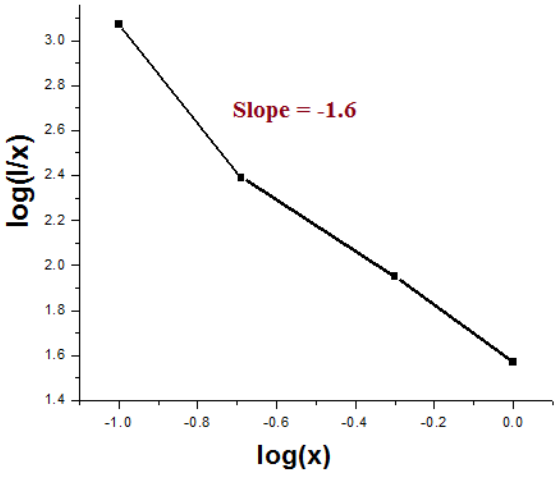

Figure 11: Plot for the emission intensity per Dy ions as a function of Dy concentration.

Critical transfer distance (R_c) in LaB_3O_6: Dy^{3+} phosphor:

In the case of investigating the concentration quenching process of Dy^{3+} ions in LaB_3O_6: Dy^{3+} phosphors, the excitation and emission spectra of phosphors with different Dy^{3+} content (x = 0.05-1 mole %) excited by 348nm are shown in figure 10 and 11. No obvious changes for all the samples in the positions of emission bands. With increasing Dy^{3+} concentration, the emission intensity increase and reaches the maximum at x = 0.1 mole %. Concentration quenching occurs, when the Dy^{3+} concentration is more than 0.1 mole %. While considering the mechanism of energy transfer in oxide phosphors, Blasse has pointed out that if the activator is introduced solely on Z ion sits, then there is on the average of one activator ion per V/xcN, where x_c is the critical concentration, N the number of Z ions in the unit cell and V the volume of the unit cell. The critical transfer distance R_c is approximately equal to twice the radius of a sphere with the volume [36].

$$R_c = 2(3V/4\pi x_c N)^{1/3} \quad \text{---------- (1)}$$

By taking the appropriate values of V, N and x_c (421.13 Å, 4, 0.001) respectively, the critical transfer distance of Dy^{3+} in LaB_3O_6: Dy^{3+} phosphor is found to be 12.39 Å.

The intensity of multipolar interaction can be determined, if the energy transfer occurs between the same sorts of activators,. The emission intensity (I) per activator ion follows the equation [36]:

$$I/x = K/1+\beta x^{Q/3} \quad \text{---------- (2)}$$

Where, x is the activator concentration; Q =3, 6, 8, 10 for the exchange interaction, dipole-dipole (d-d), dipole-quadrupole (d-q), quadrupole-quadrupole (q-q) interactions, respectively; whereas K and b are constant for a given host crystal under same excitation condition. The critical concentration of Dy^{3+} has been determined to be 0.1mole %. The dependence of the emission intensity of LaB_3O_6:Dy^{3+} phosphor excited at 348nm as a function of the corresponding concentration of Dy^{3+} for concentration greater than

the critical concentration is the determined. Equation-1, can be simply rearranged as follows:

$\log [I/x] = A-Q/3 \log x$ [$A = \log K - \log \beta$]---------(3)

Considering these equations, we had calculated and plotted log (1/x) Vs. log(x) as shown in figure 11. The value of Q can be calculated approximately as 3, this indicates that the type of interaction is the exchange interaction.

4.3.3 LaB_3O_6 Tb^{3+} phosphor

The phosphors $LaB_3O_{66}:Tb^{3+}$ with different doping concentrations of Tb^{3+} exhibit similar excitation and emission spectra except for their intensities. The excitation spectrum from 200 nm to 500 nm of $LaB_3O_6:Tb^{3+}$ (1 mole %) monitored at λ_{em}= 545 nm is shown in figure 12. The overall excitation spectrum consists of two parts. One part in the range from 250 to 300 nm is attributed to the $^4f_8 \rightarrow {}^4f_7{}^5d_1$ transition of Tb^{3+} shown in figure 12. The other part in the range of 300–500 nm contains several peaks, which can be assigned to the $^4f_8 \rightarrow {}^4f_8$ transitions from the ground state $^7F_6$ to the excitation levels such as $^5H_6$ (303 nm), $^5H_7$ or $^5D_{0,1}$ (317 nm), $^5G_2$ or $^5L_6$ (340 nm), $^5L_9$ or $^5G_4$ (351 nm), $^5L_{10}$ (368 nm), $^5G_6$ or $^5D_3$ (378 nm) and $^5D_4$ (486 nm) [37]. Among all the excitation bands, the strongest one is located in UV region (at 379 nm). Therefore, $LaB_3O_{66}:Tb^{3+}$ phosphor can be effectively excited by ultra-violet light. Figure 13 exhibits the emission spectrum of $LaB_3O_{66}:Tb^{3+}$ excited by 379 nm light. It consists of three Tb^{3+} emission peaks at 493, 545 and 588 nm, corresponding to the transitions from $^5D_4$ to $^7F_6$, $^7F_5$ and $^7F_4$ respectively, of which the green emission at 545 nm is the strongest one. The excitation and emission spectra reveals that $LaB_3O_{66}:Tb^{3+}$ is suitable for being excited by ultra-violet (at 379nm) light and produces green emission. As seen in figure 13, concentration quenching is not observed till 1mole % of Tb^{3+}.

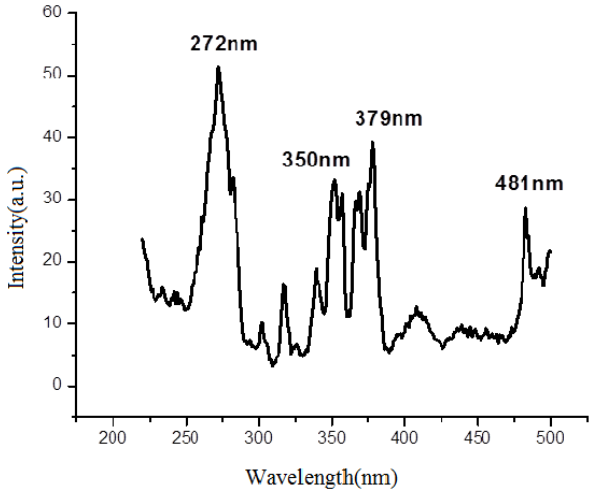

Figure 12 : Excitation spectrum of $La_{0.99}B_3O_6$: 0.01Tb monitored at λ_{em} = 545 nm.

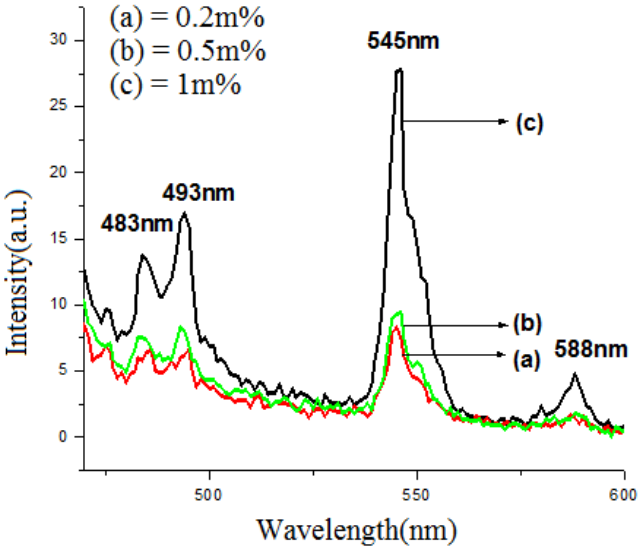

Figure 13 : Emission spectrum of La_{1-x} B_3O_6: xTb^{3+} (x= 0.2, 0.5, 1m %) monitored at λ_{exc} = 379 nm.

4.4 CIE Co-ordinates

The chromaticity co-ordinates of prepared samples were calculated using the photoluminescence data and Interactive CIE software. The calculated CIE coordinates of prepared phosphor are shown on 1931 CIE chromaticity diagram in figure 14. Figure 14 gives the chromaticity coordinates of the prepared phosphors $LaB_3O_6:Ln^{3+}$ (Ln = Eu, Dy and Tb). Chromaticity co-ordinates of $LaB_3O_6:Eu^{3+}$, $LaB_3O_6:Dy^{3+}$ and $LaB_3O_6:Tb^{3+}$ are A (x = 0.65, y = 0.33) red region, B (x = 0.31, y = 0.32) white region with correlated color temperature 6498 K and C (x = 0.33,

0.57) green region respectively. These coordinates are near to the National Television System Committee standards (x = 0.67, y = 0.33) and (x = 0.21, y = 0.71) for red and green region, respectively.

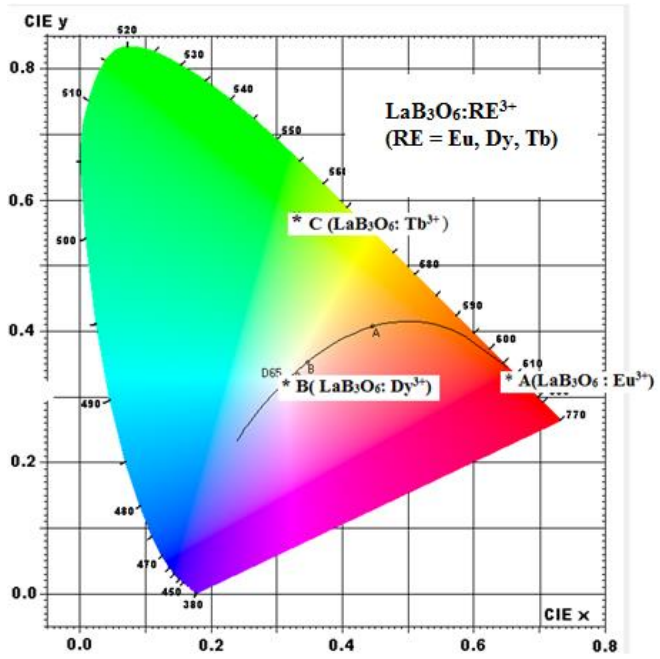

Figure 14: CIE chromaticity diagram of LaB_3O_6: Ln^{3+} (Ln = Eu, Tb, Dy), co-ordinate A of LaB_3O_6: Eu^{3+}, B of LaB_3O_6: Dy^{3+} and C of LaB_3O_6: Tb^{3+}.

V. Conclusion

The XRD pattern of LaB_3O_6: Eu phosphor matches well with those in JCPDS file no. 01-073-1150, indicating that the obtained sample is single phase. Effect of heating time during synthesis and concentration of Eu^{3+} on PL of LaB_3O_6 was investigated. Synthesis of this phosphor was done at 800°C for 24 and 48 hrs. In other case phosphor prepared for 24hrs was quenched at 800° C for 1hr. It was observed that increasing the heating time of synthesis changes the emission of Europium from blue to red i.e. Eu^{2+} to Eu^{3+}. Quenching at 800°C for 1hr also showed the same results. This phosphor gives reddish orange emission under n-UV excitation (395 nm) making it promising candidate for LED. The emission spectra of Dy^{3+}: LaB_3O_6 phosphors show two strong bands in blue and yellow regions. PL results of Dy^{3+}: LaB_3O_6 phosphor shows the excitation peak at 348nm, which is away from Hg excitation and can be useful for solid state lighting in lamp industry. LaB_3O_6 doped with Tb^{3+} have strong excitation band located at 379nm, which is suitable for being excited by user UV LED chip. It generates bright green emission at 545nm ($^5D_4 \rightarrow {}^7F_5$) under 379nm excitation. So LaB_3O_6: Tb^{3+} may be predicted as a promising green phosphor candidate for applications in LED based solid state lighting or other display devices.

VI. REFERENCES

[1]. C.M. Mehare, Y.R. Parauha, N.S. Dhoble, C. Ghanty, S.J. Dhoble, Synthesis of novel Eu2+ activated K3Ca2(SO4)3F down-conversion phosphor for near UV excited white light emitting diode, J. Mol. Struct. 1212 (2020) 127957. https://doi.org/10.1016/j.molstruc.2020.127957.

[2]. Y. Parauha, S.J. Dhoble, Synthesis and luminescence characterization of Eu3+ doped Ca7Mg2(PO4)6 phosphor for eco-friendly white LEDs and TL Dosimetric applications, Luminescence. 2 (2020). https://doi.org/10.1002/bio.3900.

[3]. Y.R. Parauha, R.S. Yadav, S.J. Dhoble, Enhanced photoluminescence via doping of phosphate, sulphate and vanadate ions in Eu3+ doped La2(MoO4)3 downconversion phosphors for white LEDs, Opt. Laser Technol. 124 (2020). https://doi.org/10.1016/j.optlastec.2019.105974.

[4]. C.H. Lin, T.Y. Li, J. Zhang, Z.Y. Chiao, P.C. Wei, H.C. Fu, L. Hu, M.J. Yu, G.H. Ahmed, X. Guan, C.H. Ho, T. Wu, B.S. Ooi, O.F. Mohammed, Y.J. Lu, X. Fang, J.H. He, Designed growth and patterning of perovskite nanowires for lasing and wide color gamut phosphors with long-term stability, Nano Energy. 73 (2020) 104801. https://doi.org/10.1016/j.nanoen.2020.104801.

[5]. S.K. Ramteke, A.N. Yerpude, N.S. Kokode, V. V. Shinde, S.J. Dhoble, Eu3+ and Dy3+-activated LaAlO3 phosphor for solid-state lighting, J. Mater.

Sci. Mater. Electron. 31 (2020) 6506–6509. https://doi.org/10.1007/s10854-020-03208-x.

[6]. R. Priya, O.P. Pandey, Structural, morphological, luminescent and magnetic studies of CTAB and TOPO assisted Gd2O3:Eu phosphors synthesized via co-precipitation route, J. Alloys Compd. 847 (2020) 156388. https://doi.org/10.1016/j.jallcom.2020.156388.

[7]. C. Growth, N.P. Company, F. Libo, THE CZOCHRALSKI GROWTH OF L1BO2 AND L12B4O7 J.D. GARRETT, M. Natarajan IYER and J.E. GREEDAN, J. Cryst. Growth. 41 (1977) 225–227.

[8]. B.V. Grinyov, Borate single crystals for polyfunctional applications: production and properties, Semicond. Physics, Quantum Electron. Optoelectron. 3 (2000) 410–419. https://doi.org/10.15407/spqeo3.03.410.

[9]. Z. Guoqing, X. Jun, C. Xingda, Z. Heyu, W. Siting, X. Ke, D. Peizhen, G. Fuxi, Growth and spectrum of a novel birefringent α-BaB2O4 crystal, J. Cryst. Growth. 191 (1998) 517–519. https://doi.org/10.1016/S0022-0248(98)00162-6.

[10]. J.W. Kim, C.S. Yoon, H.G. Gallagher, Dielectric properties of lithium triborate single crystals, Appl. Phys. Lett. 71 (1997) 3212–3214. https://doi.org/10.1063/1.120293.

[11]. J.M. Tu, D.A. Keszler, CsLiB6O10: A noncentrosymmetric polyborate, Mater. Res. Bull. 30 (1995) 209–215. https://doi.org/10.1016/0025-5408(94)00121-9.

[12]. Z.G. Hu, T. Higashiyama, M. Yoshimura, Y. Mori, T. Sasaki, Flux growth of the new nonlinear optical crystal: K2Al2B2O7, J. Cryst. Growth. 212 (2000) 368–371. https://doi.org/10.1016/S0022-0248(00)00012-9.

[13]. G. Dominiak-Dzik, W. Ryba-Romanowski, S. Goląb, L. Macalik, J. Hanuza, A. Pajączkowska, Spectroscopic investigation of Nd3+ and Yb3+ in Ca4GdO(BO3)3 crystals, J. Mol. Struct. 555 (2000) 213–225. https://doi.org/10.1016/S0022-2860(00)00604-9.

[14]. H. Zhang, X. Meng, P. Wang, L. Zhu, X. Liu, X. Liu, Y. Yang, R. Wang, J. Dawes, J. Piper, S. Zhang, L. Sun, Growth of Yb-doped Ca4GdO(BO3)3 crystals and their spectra and laser properties, J. Cryst. Growth. 222 (2001) 209–214. https://doi.org/10.1016/S0022-0248(00)00919-2.

[15]. D. Jaque, J. García Solé, Temperature decrease induced by stimulated emission in the Nd3+ ion-doped YAl3(BO3)4 crystal, Chem. Phys. Lett. 334 (2001) 309–313. https://doi.org/10.1016/S0009-2614(00)01424-X.

[16]. V. Petrov, F. Rotermund, F. Noack, R. Komatsu, T. Sugawara, S. Uda, Vacuum ultraviolet application of Li2B4O7 crystals: Generation of 100 fs pulses down to 170 nm, J. Appl. Phys. 84 (1998) 5887–5892. https://doi.org/10.1063/1.368904.

[17]. G. Corradi, V. Nagirnyi, A. Watterich, A. Kotlov, K. Polgr, Different incorporation of Cu+ and Cu2+ in lithium tetraborate single crystals, J. Phys. Conf. Ser. 249 (2010) 0–6. https://doi.org/10.1088/1742-6596/249/1/012008.

[18]. O. Legorreta-Alba, E. Cruz-Zaragoza, D. Díaz, J. Marcazzó, Synthesis of MgB4O7:Dy3+ and Thermoluminescent Characteristics at Low Doses of Beta Radiation, J. Nucl. Physics, Mater. Sci. Radiat. Appl. 6 (2018) 71–76. https://doi.org/10.15415/jnp.2018.61012.

[19]. A.H. Oza, N.S. Dhoble, S.J. Dhoble, Influence of P ion on Sr2B5O9Cl:Eu for TL dosimetry, Nucl. Instruments Methods Phys. Res. Sect. B Beam Interact. with Mater. Atoms. 344 (2015) 96–103. https://doi.org/10.1016/j.nimb.2014.12.003.

[20]. M.J. Knitel, V.R. Bom, P. Dorenbos, C.W.E. Van Eijk, I. Berezovskaya, V. Dotsenko, Feasibility of boron containing phosphors in thermal neutron image plates, in particular the systems M2B5O9X:Eu2+ (M = Ca, Sr, Ba; X = Cl, Br). Part I: simulation of the energy deposition process, Nucl. Instruments Methods Phys. Res. Sect. A

Accel. Spectrometers, Detect. Assoc. Equip. 449 (2000) 578–594. https://doi.org/10.1016/S0168-9002(99)01474-6.

[21].D.S. Thakare, S.K. Omanwar, P.L. Muthal, S.M. Dhopte, V.K. Kondawar, S. V. Moharil, UV-emitting phosphors: Synthesis, photoluminescence and applications, Phys. Status Solidi Appl. Res. 201 (2004) 574–581. https://doi.org/10.1002/pssa.200306720.

[22].K. Machida, G. Adachi, J. Shiokawa, Luminescence properties of Eu(II)-borates and Eu2+- activated Sr-Borates, J. Lumin. 21 (1979) 101–110. https://doi.org/10.1016/0022-2313(79)90038-3.

[23].G.B.C. Blasse G., A General Introduction to Luminescent Materials, Luminescen, Springer, Berlin, Heidelberg., 1994. https://doi.org/10.1007/978-3-642-79017-1_1.

[24].C. De Bellevue, Crystal Growth and Characterization of InBO3:Tb3+, J. Cryst. Growth. 99 (1990) 799–804.

[25].I.E. Kwon, B.Y. Yu, H. Bae, Y.J. Hwang, T.W. Kwon, C.H. Kim, C.H. Pyun, S.J. Kim, Luminescence properties of borate phosphors in the UV/VUV region, J. Lumin. 87 (2000) 1039–1041. https://doi.org/10.1016/S0022-2313(99)00532-3.

[26].Y. Zhang, Z. Lin, Z. Hu, G. Wang, Growth and spectroscopic properties of Nd3+-doped Sr3Y2(BO3)4 crystal, J. Solid State Chem. 177 (2004) 3183–3186. https://doi.org/10.1016/j.jssc.2004.04.017.

[27].S. Filatov, Y. Shepelev, R. Bubnova, N. Sennova, A. V. Egorysheva, Y.F. Kargin, The study of Bi3B5O12: Synthesis, crystal structure and thermal expansion of oxoborate Bi3B5O12, J. Solid State Chem. 177 (2004) 515–522. https://doi.org/10.1016/j.jssc.2003.03.003.

[28].X. Chen, M. Li, X. Chang, H. Zang, W. Xiao, Synthesis and crystal structure of a novel pentaborate, Na3ZnB5O10, J. Solid State Chem. 180 (2007) 1658–1663. https://doi.org/10.1016/j.jssc.2007.03.014.

[29].A.M. Srivastava, M.G. Brik, The dependence of 10 Dq crystal field parameter for Mn4+ (3d3 configuration) and the magnitude of 7F1 level splitting for Eu3+ (4f6 configuration) on pyrochlore compositions, Opt. Mater. (Amst). 35 (2012) 196–200. https://doi.org/10.1016/j.optmat.2012.07.026.

[30].S.R. Bargat, Y.R. Parauha, G.C. Mishra, S.J. Dhoble, Combustion synthesis and spectroscopic investigation of CaNa2(SO4)2:Eu3+ phosphor, J. Mol. Struct. 1221 (2020) 128838. https://doi.org/10.1016/j.molstruc.2020.128838.

[31].P.A. Tanner, Some misconceptions concerning the electronic spectra of tri-positive europium and cerium, Chem. Soc. Rev. 42 (2013) 5090–5101. https://doi.org/10.1039/c3cs60033e.

[32].R.R. Carnall W., Goodmen G., Rajnak K., A systematic analysis of the spectra of the lanthanides doped into single crystal LaF3, J. Chem. Phys. 90 (1989) 3443.

[33].Y.R. Parauha, V. Chopra, S.J. Dhoble, Synthesis and luminescence properties of RE3+ (RE= Eu3+, Dy3+) activated CaSr2(PO4)2 phosphors for lighting and dosimetric applications, Mater. Res. Bull. 131 (2020) 110971. https://doi.org/10.1016/j.materresbull.2020.110971.

[34].X. Liu, R. Pang, Q. Li, J. Lin, Host-sensitized luminescence of Dy3+, Pr3+, Tb3+ in polycrystalline CaIn2O4 for field emission displays, J. Solid State Chem. 180 (2007) 1421–1430. https://doi.org/10.1016/j.jssc.2007.01.034.

[35].Z. Xiu, Z. Yang, M. Lü, S. Liu, H. Zhang, G. Zhou, Synthesis, structural and luminescence properties of Dy3+-doped YPO4 nanocrystals, Opt. Mater. (Amst). 29 (2006) 431–434. https://doi.org/10.1016/j.optmat.2005.08.038.

[36].Yatish R. Parauha, S.J.Dhoble, Photoluminescence and electron-vibrational interaction in 5d state of

Eu2+ ion in Ca3Al2O6 down-conversion phosphor, Opt. Laser Technol. 142 (2021) 107191. https://doi.org/10.1016/j.optlastec.2021.107191.

[37].N. Baig, J.G. Mahakhode, P. Kumari, Y.R. Parauha, N.S. Dhoble, S.B. Dhoble, Photoluminescence properties of wet-chemically synthesized Tb3+ and Sm3+ doped K3Ca2(SO4)3Cl phosphor, J. Phys. Conf. Ser. 1913 (2021) 012025. https://doi.org/10.1088/1742-6596/1913/1/012025.